

Manuscript version: Author's Accepted Manuscript

The version presented in WRAP is the author's accepted manuscript and may differ from the published version or Version of Record.

Persistent WRAP URL:

<http://wrap.warwick.ac.uk/127809>

How to cite:

Please refer to published version for the most recent bibliographic citation information. If a published version is known of, the repository item page linked to above, will contain details on accessing it.

Copyright and reuse:

The Warwick Research Archive Portal (WRAP) makes this work by researchers of the University of Warwick available open access under the following conditions.

© 2019 Elsevier. Licensed under the Creative Commons Attribution-NonCommercial-NoDerivatives 4.0 International <http://creativecommons.org/licenses/by-nc-nd/4.0/>.

**Publisher's statement:**

Please refer to the repository item page, publisher's statement section, for further information.

For more information, please contact the WRAP Team at: wrap@warwick.ac.uk.

1 **Early cortical surface plasticity relates to basic mathematical learning**

2 Running title: Early cortical plasticity relates to math learning

3

4 Ulrike Kuhl^{a*}, Angela D. Friederici^a, the LEGASCREEN consortium^{a,b} & Michael A. Skeide^a

5 ^a Department of Neuropsychology, Max Planck Institute for Human Cognitive and Brain

6 Sciences, Stephanstraße 1a, 04103 Leipzig, Germany.

7 ^b Fraunhofer Institute for Cell Therapy and Immunology, Perlickstr. 1, 04103 Leipzig,

8 Germany.

9

10 *Corresponding author:

11 Ulrike Kuhl, MSc

12 Max Planck Institute for Human Cognitive and Brain Sciences

13 Stephanstr. 1a

14 04103 Leipzig

15 Germany

16 kuhl@cbs.mpg.de

17 Phone: +49 341 9940-2625

- 18 Number of pages: **42**
- 19 Number of figures: 2
- 20 Number of tables: 2
- 21 Number of supplementary tables: 5
- 22 Number of words for Abstract: 209
- 23 Number of words for Introduction: **1406**
- 24 Number of words for Discussion: **2073**

25 **Abstract**

26 Children lay the foundation for later academic achievement by acquiring core mathematical
27 abilities in the first school years. Neural reorganization processes associated with individual
28 differences in early mathematical learning, however, are still poorly understood. To fill this
29 research gap, we followed a sample of 5-6-year-old children longitudinally to the end of second
30 grade in school (age 7-8 years) combining magnetic resonance imaging (MRI) with
31 comprehensive behavioral assessments. We report significant links between the rate of
32 neuroplastic change of cortical surface anatomy, and children's early mathematical skills. In
33 particular, most of the behavioral variance (about 73%) of children's visuospatial abilities was
34 explained by the change in cortical thickness in the right superior parietal cortex. Moreover,
35 half of the behavioral variance (about 55%) of children's arithmetic abilities was explained by
36 the change in cortical folding in the right intraparietal sulcus. Additional associations for
37 arithmetic abilities were found for cortical thickness change of the right temporal lobe, and the
38 left middle occipital gyrus. Visuospatial abilities were related to right precentral and
39 supramarginal thickness, as well as right medial frontal gyrus folding plasticity. These effects
40 were independent of other individual differences in IQ, literacy and maternal education. Our
41 findings highlight the critical role of cortical plasticity during the acquisition of fundamental
42 mathematical abilities.

43 **Keywords:** mathematical learning; visuospatial quantity processing; arithmetic; parietal
44 cortex; brain development; gray matter

45 **Highlights:**

- 46 • MRI study of cortical plasticity during first years of formal math instruction
- 47 • Right superior parietal thickness change was related to visuospatial processing
- 48 • Right intraparietal sulcus folding plasticity was related to early arithmetic
- 49 • Left occipital, and right fronto-temporal regions showed further associations
- 50 • Results link cortical plasticity to basic math learning

51 **1. Introduction**

52 Mathematical abilities are crucial for everyday life, enabling us to find the right page in a book,
53 schedule appointments or do financial transactions. Moreover, early mathematical skills are
54 among the strongest predictors of academic achievement (Duncan et al., 2007).

55 Infants as young as 6 months already show an intuitive sense for magnitude (Dehaene, 2011;
56 Xu and Spelke, 2000). This visceral understanding of numerosity increases in precision over
57 development (Lipton and Spelke, 2003), eventually enabling preschoolers to perform
58 approximate addition (Barth et al., 2006, 2005) and subtraction (Slaughter et al., 2006) based
59 on visuospatial representation of magnitude. However, children acquire the skills needed for
60 exact symbolic arithmetic not until it is formally taught in school (Barth et al., 2005). During
61 these developmental trajectories individuals show marked variability in growth of knowledge
62 (Brown et al., 2003; Cockcroft, 1982).

63 **Mature** mathematical problem-solving involves working memory, cognitive control, attention,
64 memory, visual processing, and numerical cognition (Menon, 2015). **Importantly,**
65 **developmental studies highlight a specific association between visuo-spatial processing,**
66 **including visuo-spatial working memory, and emerging mathematical performance (Bull**
67 **et al., 2008). This relationship, however, decreases quickly already during the first two**
68 **years of school (De Smedt et al., 2009). A possible explanation for this change might be a**
69 **shift from initially relying on visuo-spatial representations of magnitude and problem-**
70 **solving strategies like finger counting (Rasmussen and Bisanz, 2005) to verbal retrieval**
71 **strategies (De Smedt et al., 2009).**

72 **Considering this the heterogenous nature of mathematical problem-solving, it is not**
73 **surprising that** a diverse range of brain regions has been associated with its development,
74 including prefrontal cortex (PFC; Rivera et al., 2005; Cho et al., 2011; Evans et al., 2015) and
75 the medial temporal lobe (MTL; Rivera et al., 2005; Cho et al., 2011; Supekar et al., 2013; Qin

76 et al., 2014), ventral temporal-occipital cortex (VTOC; Evans et al., 2015; Rivera et al., 2005),
77 encompassing a putative number-form area (Nemmi et al., 2018), temporo-parietal regions
78 including the angular and supramarginal gyri (AG, SMG; Peters et al., 2016; Peters and De
79 Smedt, 2018; Price et al., 2013) and posterior parietal cortex (PPC; Rivera et al., 2005; Cantlon
80 et al., 2006; Menon, 2010; Qin et al., 2014), including the intraparietal sulcus (IPS; Cantlon et
81 al., 2006; Emerson and Cantlon, 2015; Jolles et al., 2016a; Schel and Klingberg, 2017).

82 Importantly, previous studies demonstrate characteristic structural and functional changes
83 within these regions while mathematical competence refines, both in terms of visuospatial
84 magnitude processing and arithmetic abilities. In line with accounts of a ventro-temporal region
85 specialized for the processing of numerals in adults (Hannagan et al., 2015; Yeo et al., 2017),
86 differential functional connectivity between the VTOC and the IPS emerges already at three
87 years of age, before children encounter formal mathematical education (Nemmi et al., 2018).

88 Further, gradual increases in mathematical ability are associated with increasing functional
89 connectivity of numeral-selective areas to parietal and prefrontal regions during early
90 adolescence (Nemmi et al., 2018). Moreover, activation of prefrontal regions decreases during
91 development, reflecting reduced reliance on working memory and attentional resources. At the
92 same time, involvement of the IPS, SMG and anterior AG increases (Rivera et al., 2005),
93 follows a regionally specific pattern: activation during numerical problem solving increases
94 linearly in ventral IPS, anterior AG and the posterior SMG from child- to adulthood, reflecting
95 the specialization of these areas for mathematical processing with time and experience (Chang
96 et al., 2016; Rivera et al., 2005). Activation in anterior segments of the SMG, in contrast, peaks
97 in adolescence before declining again towards adulthood (Chang et al., 2016).

98 In adults, the IPS and also the PPC are associated with representing and manipulating symbolic
99 as well as non-symbolic magnitude (Piazza et al., 2007, 2006, 2004) and mental arithmetic
100 (Knops et al., 2009; Menon et al., 2000; Venkatraman et al., 2005). Due to their specific
101 involvement in symbolic numerical processing as compared to processing of non-symbolic

102 visual magnitude (Peters et al., 2016), AG and SMG have been linked to the retrieval of
103 arithmetic and numerical fact knowledge from long-term memory (Peters and De Smedt, 2018).
104 In line with this notion, activity in AG and SMG has been shown to correlate with arithmetic
105 expertise in adults (Grabner et al., 2007), a pattern that has also been found in adolescents (Price
106 et al., 2013).

107 In six year old children, both first mathematical abilities and visuospatial working memory are
108 associated with cortical thickness of the anterior portion of the right IPS (Schel and Klingberg,
109 2017). In line with this, the longitudinal change in parietal gray matter volume, alongside
110 ventro-temporal and prefrontal regions, predicts longitudinal gain in mathematical competence
111 in children between 7 and 14 years of age (Evans et al., 2015).

112 Specific brain areas have been linked to visuo-spatial magnitude processing at a preschool age
113 (Cantlon et al., 2006) and mathematical development at a school age (Evans et al., 2015; Qin
114 et al., 2014; Rivera et al., 2005). However, little is known about the neural correlates of
115 emerging mathematical abilities during the first years of formal instruction in school. This is a
116 substantial research gap, since, during this time, children move from approximate to exact
117 calculation (Cho et al., 2011). Therefore, we investigated changes of cortical surface anatomy
118 in children at the transition from kindergarten to second grade and related them to their
119 mathematical performance. Recent evidence supports the notion that arithmetic and
120 visuospatial magnitude processing, two important components of mathematical competence,
121 are indeed supported by distinct cognitive processes. Specifically, Georges et al. (2017) found
122 that arithmetic problem-solving abilities - but not visuospatial magnitude processing abilities -
123 relate strongly to spatially-organized representations of number. In line with this, we expect
124 different components of numerical cognition to be supported by different brain structures,
125 reflected by relationships between structural change and early mathematical ability.

126 Links between distinct developmental trajectories of cortical anatomical measures and variable
127 performance with respect to higher cognitive functioning have been revealed in previous work

128 (Raznahan et al., 2011; Schnack et al., 2015). For instance, Schnack et al. (2015) related faster
129 rates of left-sided cortical thinning from child- to early adulthood with higher intelligence.
130 Changes in cortical surface morphometry may be traced back to cellular processes affecting the
131 cortical cytoarchitecture, like neuro-, glio- and synaptogenesis, synaptic pruning or progressive
132 growth of deep cortical white matter (Natu et al., 2018; Zatorre et al., 2012). Therefore,
133 systematic associations between behavior and the brain's surface-based trajectories might
134 indicate changes in terms of efficiency of brain networks relevant for higher cognitive
135 functioning (Bullmore and Sporns, 2012).

136 It is noteworthy that classical voxel-based morphometry analyses capture information of grey
137 matter volume only, thus conflating information from distinct morphometric properties.
138 Specifically, cortical volume is a composite of the thickness of the cortical ribbon and the area
139 of its surface. This areal expansion, in turn, is reflected by degree and shape of cortical
140 convolutions (Raznahan et al., 2011). Specifically, sustained growth of the outer cortical
141 surface driven by continued maturation of neurons and their connectivity (Budday et al., 2015a;
142 Richman et al., 1975) gives rise to a greater number of cortical folds and deeper sulci. Thus,
143 while previous work focusing either on gray matter volume or cortical thickness cannot
144 disentangle differences driven by cortical thickness and folding (Mechelli et al., 2005), our goal
145 was to go beyond these traditional indices and further explore gyrification, cortical folding
146 regularity and sulcus depth.

147 All analyses were controlled for prominent behavioral correlates in order to be able to draw
148 specific conclusions about cortical development and mathematical ability. To this end,
149 measures assessing reading and spelling ability, sociodemographic status, non-verbal IQ,
150 handedness, sex and age served as covariates in the statistical models. Given that deficits in
151 literacy and mathematical development are reported to frequently co-occur (Dirks et al.,
152 2008; Moll et al., 2014), familial risk of developing dyslexia was also taken into account in
153 the current work.

154 **The aim of the current work was to identify distinct** anatomical correlates of individual
155 differences **in two important subcomponents of** early mathematical **skill, i.e., visuo-spatial**
156 **magnitude processing and arithmetic abilities. We expected to find associations between**
157 **early visuo-spatial magnitude processing abilities and structural reorganization processes**
158 **within the IPS and the PPC, given their involvement in visuo-spatial imagery, and within**
159 **prefrontal regions supporting visuospatial working memory (Formisano et al., 2002;**
160 **Klingberg, Forssberg, & Westerberg, 2002; Kwon, Reiss, & Menon, 2002)”. Further, we**
161 **expected to find associations between arithmetic processing and regions known to**
162 **represent numerical information, i.e. the IPS and the PPC, and the hippocampus as a**
163 **region involved in arithmetic fact retrieval.**

164 **2. Materials and Methods**

165 *2.1. Participants*

166 Children were recruited from the Leipzig metropolitan area between 2012 and 2013. Initial data
167 acquisition and screening for neurological, psychiatric, hearing or vision disorders took place
168 between 2012 and 2013. Follow-up sessions were conducted between 2015 and 2016. Twenty-
169 eight native German, monolingual children completed the study (15 female; age range at
170 kindergarten: 5 years, 0 months – 6 years, 0 months; mean \pm SD: 5 years, 6 months \pm 6 months;
171 age range at second grade in school: 7 years, 11 months – 8 years, 11 months; mean \pm SD: 8
172 years, 5 months \pm 5 months). Fifty-four other children participated but were excluded from
173 further analysis because they received a diagnosis of attention deficit hyperactivity disorder
174 (n=4) or developmental dyslexia (n=9, both determined based on parental questionnaire), did
175 not have complete datasets (i.e., did not comply with the experimental procedures in a training
176 session, were unable to attend follow-up sessions, or exhibited imaging data corrupted by
177 artifacts, n=22), did not complete all psychometric tests (n=3), scored below the 20th percentile
178 rank of the population performance in standardized and age-normed reading or spelling tests

179 (n=12) or performed below the 20th percentile in a standardized math test (clinical cases of
180 developmental dyscalculia, n=3). One additional child had to be excluded due to an
181 experimental error during psychometric testing. None of the remaining children scored below
182 85 on average in two non-verbal IQ tests. The study was approved by the Ethics Committee of
183 the University of Leipzig, Germany. Written informed consent was obtained from parents and
184 children gave verbal informed assent.

185 *2.2. Psychometric assessment*

186 Children's mathematical ability at the end of second grade in school was quantified using the
187 Heidelberg computation test (HRT; Haffner et al., 2005). The HRT includes two subscales. The
188 first subscale quantifies children's early arithmetic abilities with subtests requiring simple
189 addition and subtraction, solving simple equations and performing greater-or-smaller-than
190 comparisons. The second subscale assesses children's visuospatial skills, providing a composite
191 score of tasks that require children to estimate the length of line-drawings and the number of
192 cubes needed for cube structures, to count shapes in a visual array, to connect spatially
193 scrambled numerals in ascending order and to extract the rule determining the sequence of a
194 given row of numbers.

195 All children underwent additional psychometric assessment at both kindergarten and school
196 age. At kindergarten age, we assessed children's non-verbal intelligence using the Wechsler
197 preschool and primary scale of intelligence (Wechsler et al., 2009) and their handedness
198 (Oldfield, 1971). At the end of second grade, we assessed children's spelling accuracy focusing
199 on writing after dictation of words in the German spelling test (Stock and Schneider, 2008). We
200 also examined reading fluency based on number of words correctly read within 1 minute as part
201 of the German Salzburg test of reading and spelling (Moll and Landerl, 2010). Non-verbal
202 intelligence was assessed using the Wechsler Intelligence Scale for children (WISC-IV;
203 Petermann and Petermann, 2011).

204 2.3. Sociodemographic measures

205 The highest level of education (4-point scale ranging from 0 = no degree to 3= German ‘Abitur’
206 [high school diploma / A level]) and vocational qualification (5-point scale ranging from 0 =
207 no qualification to 4 = German ‘Habilitation’ [postdoctoral academic qualification]) was
208 obtained from each parent and/or primary caregiver using a questionnaire. In the final sample,
209 maternal education ranged from 2 to 7 (mean \pm SD = 4.43 \pm 0.51).

210

211 2.4. MRI data acquisition

212 At kindergarten age, a training session using a mock scanner was conducted to familiarize
213 children with the MRI procedure and to maximize compliance. In a subsequent session,
214 scanning was performed on a 3 T Siemens TIM Trio magnetic resonance scanner (Siemens AG,
215 Erlangen, Germany) with a 12 channel radio-frequency head coil. T1 maps were acquired using
216 the magnetization-prepared 2 rapid acquisition gradient echo (MP2RAGE, Marques et al.,
217 2010) method with the following parameters: TR = 5000ms; T11/TI2 = 700/2500ms; TE =
218 2.82ms; FOV = 250 x 219 x 188mm; voxel size = 1.3mm³; GRAPPA factor = 3.

219 A second MRI session was performed at the end of second grade on the same scanner upgraded
220 to a 3T Prisma system, using a 64 channel head coil and an MP2RAGE sequence with
221 parameters TR = 5000ms; T11/TI2 = 700/2500ms; TE = 2.01ms; FOV = 256x240x176mm;
222 voxel size = 1.0mm³; GRAPPA factor = 2.

223 **Please note that we also acquired diffusion-weighted MRI as well as resting-state fMRI**
224 **for both timepoints, but after quality control these data were only available for a subset**
225 **of our final sample (diffusion-weighted MRI: n=24; resting-state fMRI: n=16).**

226 2.5. MRI preprocessing and analysis

227 Initially, T1-weighted (T1) brain images of both time points were visually inspected to exclude
228 corrupted data caused by imaging artifacts such as ghosting, Gibbs artifact or diffuse image
229 noise along the phase-encoding direction induced by excessive motion in the scanner. All
230 participants that were retained for further analysis had an overall image quality of at least
231 86% (weighted image quality rating provided by CAT12) at both timepoints. Subsequently,
232 brain images were extracted using Freesurfer (Version 5.3.0,
233 <http://surfer.nmr.mgh.harvard.edu/>). After spatially normalizing the images to a pediatric
234 template derived from 82 children aged 4.5–8.5 years (Fonov et al., 2009) in Montreal
235 Neurological Institute (MNI) stereotactic space, a common group template based on all
236 individual T1 images in MNI space from both timepoints was created with the Advanced
237 Normalization Tools (ANTs; Avants et al., 2010, 2011).

238 Using the Computational Anatomy Toolbox (CAT12, <http://www.neuro.uni-jena.de/cat/>) for
239 SPM12 (www.fil.ac.uk/spm/) in Matlab R2017b (The Mathworks, Inc., Natick, MA, USA), T1
240 data in template space were segmented into gray and white matter. For segmentation, SPM
241 relies on anatomical priors provided as tissue probability maps. Since the tissue priors provided
242 as a standard are derived from adult data, we replaced them with custom tissue probability
243 maps. These maps were derived from the common group template of both timepoints to account
244 for the anatomical details of our developmental sample, following the methodology described
245 in Cafiero et al. (2018). Probabilistic maps of the individual tissue types were created using
246 FSL's fast (Zhang et al., 2001). Tissue probabilities were normalized to sum to one. Finally, all
247 maps were resampled to a resolution of 1.5mm isotropic and smoothed using a 35mm FWHM
248 kernel, to approximate the resolution and smoothness of SPM's default anatomical priors.
249 Additionally, gray and white matter maps created this way were also used to replace the default
250 DARTEL template. During segmentation, surface-based maps of cortical thickness (CT),
251 gyrification index (GI; Lüdgers et al., 2006), cortical folding regularity (CF; Yotter et al., 2011)
252 and sulcus depth (SD) were extracted for each participant. Thickness data were smoothed with

253 a 15mm FWHM kernel, and folding, gyrification and sulcus depth data were smoothed with a
 254 20mm FWHM kernel, in accordance with the matched-filter theorem.
 255 We performed a region of interest (ROI) based analysis focused on areas previously linked to
 256 mathematical processing in adults and children to examine the relation between developmental
 257 changes in measures of cortical surface morphometry and early mathematical ability. ROIs
 258 included the bilateral IPS (Chang et al., 2016; He et al., 2014; Masataka et al., 2007), AG,
 259 SMG, hippocampus (HIP), dorso-lateral prefrontal cortex (DLPFC), ventral temporal-occipital
 260 cortex (VTOC), and bilateral visual word form area (VWFA). ROIs were derived from a multi-
 261 modal parcellation (MMP) of brain areas (Glasser et al., 2016) comprising 180 cortical regions
 262 per hemisphere (Supplementary Table S1, Figure 1a). In order to obtain participant-specific
 263 surface-based masks, the MMP (Glasser et al., 2016) was first spatially aligned with each
 264 child's MNI-T1 volumetric image and then mapped to the individual surface using the 'Map
 265 volume (Native Space) to individual surface' function in CAT12. The resulting ROIs in
 266 individual surface space were then used to mask the individual, smoothed CT, GI, SD and CF
 267 maps and extract participant-specific ROI means of all measures for both timepoints. To
 268 quantify the raw cortical change from kindergarten to second grade in school, the extracted
 269 mean values of timepoint 1 (kindergarten) were subtracted from the respective means derived
 270 from timepoint 2 (school), creating measures of Δ_{CT} , Δ_{GI} , Δ_{CF} and Δ_{SD} for each participant and
 271 each ROI. Based on these difference measures, the relative change rate R_Q (Schnack et al.,
 272 2015) for each quantity Q was computed as

$$273 \quad R_Q = \left(\frac{\Delta_Q}{(Age_{time\ 2} - Age_{time\ 1}) \times \frac{Q_{time\ 1} + Q_{time\ 2}}{2}} \right) \times 100$$

274 These relative change rates include not only the raw anatomical change but also control for
 275 the individual variance of measures at time point 1 and 2.

276 Additionally, we performed whole-brain analyses in order to make sure not to overlook effects
 277 outside of our pre-defined ROIs. To this end, we created an additional set of individual

278 templates for each child (Cafiero et al., 2018), based on the respective individual T1 MNI
279 images using ANTs. The purpose of using individual templates was to ensure optimal alignment
280 of data for both timepoints. The individual T1-images were spatially aligned to the respective
281 child's template before segmentation and the surface-based measures were extracted as
282 explained above. For each child, whole-brain maps of relative change rates (R_{CT} , R_{GI} , R_{CF} and
283 R_{SD}) as basis for whole-brain statistical analyses were computed following the formula above
284 (Schnack et al., 2015).

285 *2.6. Experimental design and statistical analysis*

286 MRI measurements and psychometric assessment were obtained from children once at
287 kindergarten, before they underwent formal mathematics instruction, and again approximately
288 2 years and 11 months later at the end of second grade.

289 Correlations between sociodemographic and psychometric measures within each time point as
290 well as across time, when suitable, were computed using R-3.3.1 (R Core Team, 2016).

291 ROI-wise partial correlations of the z-transformed relative change rates R_{CT} , R_{GI} , R_{CF} and R_{SD}
292 and HRT subscales were computed using R-3.3.1 (R Core Team, 2016). Confounding variables
293 included in the models were age at time 1, sex, handedness, non-verbal IQ at time 2, maternal
294 education, spelling accuracy, reading speed, and familial risk of developing dyslexia.
295 Additionally, to investigate the relation between brain maturation and the subscales of the test
296 in a specific fashion, we added the respective other subscale score as a covariate. Further, as
297 anatomical change measures correlate highly with size of measures at time 1, mean CT, GI,
298 CF and SD of the respective hemisphere were used as covariates when analyzing R_{CT} , R_{GI} ,
299 R_{CF} and R_{SD} respectively. To control for multiple comparisons in the ROI-based analysis, we
300 **used the Holm-Bonferroni method (Holm, 1979) at an unadjusted level of 0.05, accounting**
301 **for number of ROIs (14) and number of HRT subscales (2). Consequently, the initial critical**
302 **α level was set to 0.0018.**

303 Whole-brain correlations of individual relative change and math test (HRT) subscales were
 304 computed in SPM12. These correlations were corrected for the same confounding variables
 305 stated above. Clusters were considered significant and reported when exceeding a voxel-level
 306 threshold of $p < 0.001$ (uncorrected), with family-wise-error (FWE) correction for multiple
 307 spatial comparisons at the cluster level ($p < 0.05$).

308 **Table 1. Demographic information and psychometric test scores.**

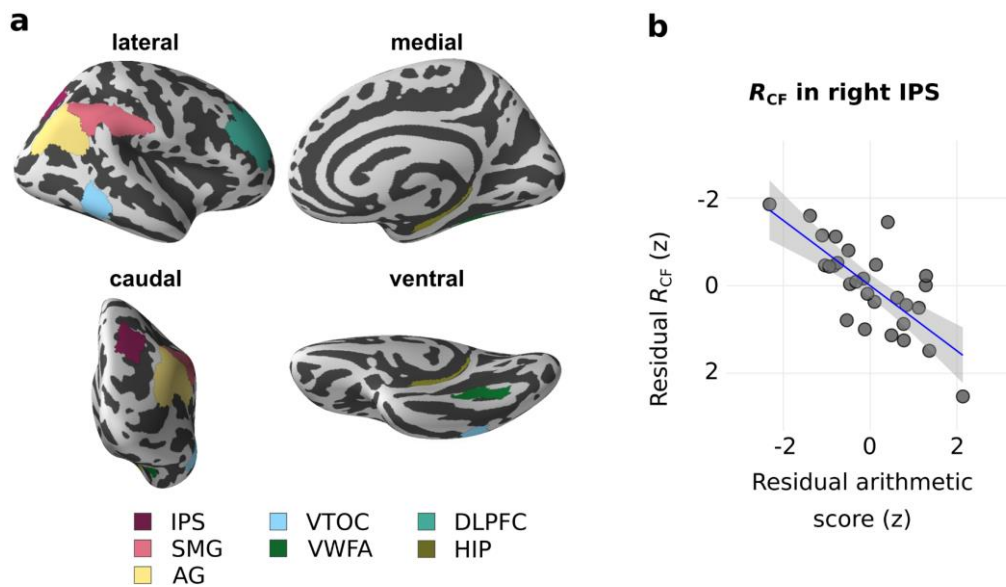
| Demographics | <i>kindergarten</i> | <i>end of second grade</i> |
|-------------------------------------|---------------------|----------------------------|
| N | 28 | .. ^d |
| Age ^a | 5;6±6 | 8;5±5 |
| Sex ^b | 13/15 | .. ^d |
| Maternal education ^c | 4.43±0.51 | .. ^d |
| Handedness ^e | 58.11±44.63 | .. ^d |
| Psychometrics | | |
| Non-verbal IQ ^f | 104.61±11.54 | 113.64±11.83 |
| Arithmetic abilities ^g | .. ^h | 69.64±23.17 |
| Visuospatial abilities ⁱ | .. ^h | 77.00±20.00 |
| Spelling accuracy ^j | .. ^h | 52.39±24.33 |
| Reading speed ^k | .. ^h | 63.71±24.96 |

^amean age: years; months ± standard deviation
^bmale/female
^cquestionnaire-derived, combined score of mother's school education (4-point scale: no degree – 0 points; German 'Abitur' [high school diploma / A level] – 3 points) and vocational qualification (5-point scale: no qualification – 0 points; German 'Habilitation' [postdoctoral academic qualification] – 4 points); mean ± standard deviation
^d data were identical for both timepoints
^e laterality quotient (LQ): mean ± standard deviation; scores range from -100 (left handed) to 100 (right handed), left-handedness: LQ < -28, i.e. the first decile value; right-handedness: LQ > 48, i.e. the first decile value; ambidexterity: -28 < LQ < 48
^f mean ± standard deviation; average normed IQ score is 100 with a standard deviation of ± 15
^g percentile ranks: mean ± standard deviation; subscale of standardized math test (HRT) comprising addition, subtraction, solving simple equation and greater-or-smaller-than-comparison tasks
^h data were only available at second timepoint
ⁱ percentile ranks: mean ± standard deviation; subscale of standardized math test (HRT) comprising tasks assessing length and magnitude estimation, counting, and numerical rule extraction abilities
^j percentile ranks: mean ± standard deviation; writing after dictation
^k percentile ranks: mean ± standard deviation; number of words correctly read within 1 minute

309 3. Results

310 Information on participants and their performance in psychometric testing is provided in Table
 311 1. There were no significant correlations between any of the sociodemographic and
 312 psychometric measures for each time point, as well as across time (Supplementary Tables S2,
 313 S3 and S4).

314 In the ROI-based analysis, we found a significant negative correlation of change rate in cortical
 315 folding regularity and the arithmetic ability subscale within the right IPS ($R^2(16) = 0.55$, $p =$
 316 0.0004 , Figure 1b). No significant correlations were observed between any other ROI and
 317 measure (Supplementary Table S5).



318

319 **Figure 1. Region-of-interest (ROI) analysis.** (a) Only right-hemispheric ROIs are depicted,
 320 but bilateral ROIs were used in the analysis. IPS = intraparietal sulcus; SMG = supramarginal
 321 gyrus; AG = angular gyrus; VTOC = ventral temporal-occipital cortex; VWFA = visual word
 322 form area; DLPFC = dorso-lateral prefrontal cortex; HIP = hippocampus. (b) A significant
 323 negative correlation (blue) was found between the residual mean R_{CF} within the right IPS and
 324 the residual arithmetic ability score ($p < 0.05$, family-wise-error corrected for the number of
 325 behavioral measures and ROIs). (b) The scatterplot denotes the association of residualized
 326 change in cortical folding regularity and z-scored arithmetic test score after accounting for age
 327 at kindergarten, sex, handedness, non-verbal IQ at the end of second grade, maternal education,
 328 spelling accuracy, reading speed, familial risk of developing dyslexia, visuospatial performance
 329 score, and mean CF at kindergarten age. The shaded area surrounding the regression line shows
 330 the 95% confidence interval. R_{CF} = change rate of cortical folding regularity.

331 The whole-brain analysis revealed significant relations between cortical change rates and
 332 mathematical test subscales (Table 2, Figure 2). Specifically, change in cortical thickness was
 333 negatively correlated with arithmetic abilities in the right temporal pole (TP; $R^2(16) = 0.52$, p
 334 $= 0.0330$) as well as left middle occipital gyrus (MOG; $R^2(16) = 0.52$, $p = 0.0300$) and positively
 335 correlated with visuospatial abilities in clusters in the right superior parietal cortex (SPL; $R^2(16)$
 336 $= 0.73$, $p < 0.0010$), two clusters within the right supramarginal gyrus (SMG; $R^2(16) = 0.40$, p

337 = 0.0440; $R^2(16) = 0.45$, $p = 0.0480$), and right postcentral gyrus ($R^2(16) = 0.51$, $p = 0.0060$).

338 Additionally, change in cortical folding regularity was negatively correlated with visuospatial

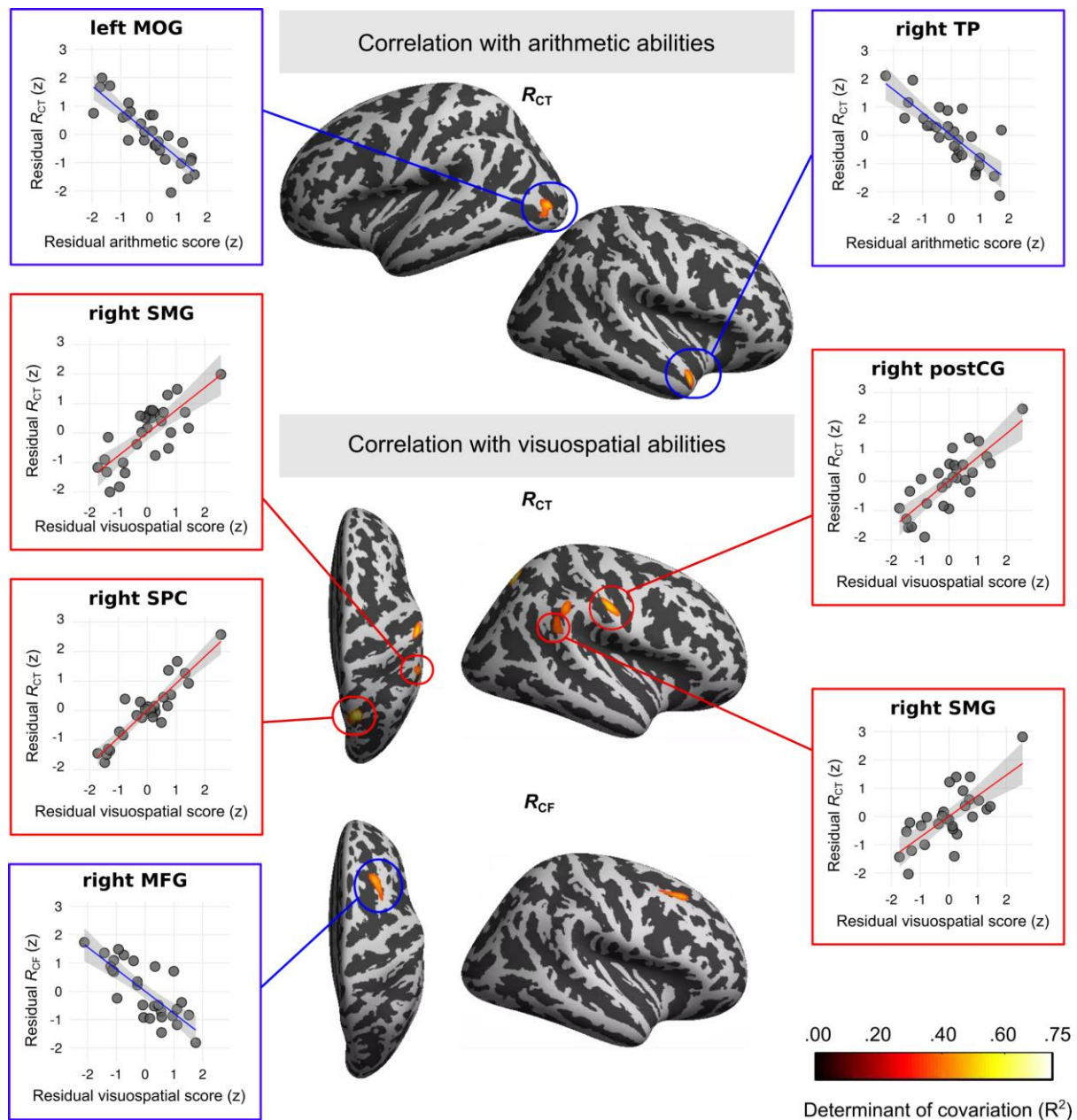
339 skills in the right middle frontal gyrus (MFG; $R^2(16) = 0.47$, $p = 0.0340$).

340

341 **Table 2. Cluster results of the whole brain vertex wise analysis.**

| Location | Coordinates | | | Size ^a | R ² | P |
|-------------------------------|-------------|-----|-----|-------------------|----------------|--------|
| | X | Y | Z | | | |
| Arithmetic abilities | | | | | | |
| <i>R_{CT}</i> | | | | | | |
| R temporal pole | 50 | 14 | -24 | 321 | 0.52 | 0.0330 |
| L middle occipital gyrus | -40 | -84 | 4 | 318 | 0.52 | 0.0300 |
| Visuospatial abilities | | | | | | |
| <i>R_{CF}</i> | | | | | | |
| R middle frontal gyrus | 29 | 20 | 45 | 376 | 0.47 | 0.0340 |
| <i>R_{CT}</i> | | | | | | |
| R superior parietal cortex | 17 | -66 | 54 | 576 | 0.73 | 0.0010 |
| R postcentral gyrus | 58 | -14 | 41 | 452 | 0.51 | 0.0060 |
| R supramarginal gyrus | 56 | -46 | 23 | 297 | 0.40 | 0.0440 |
| | 57 | -41 | 39 | 291 | 0.45 | 0.0480 |

^asize in vertices; *R_{CT}* = change in cortical thickness; *R_{CF}* = change in cortical folding regularity.



342

343 **Figure 2. Whole-brain analysis results.** Overview of clusters denoting significant partial correlations.
 344 Residual arithmetic score was significantly and negatively correlated (blue) with residual R_{CT} within a
 345 cluster in the right temporal pole and middle occipital gyrus (top row). Residual visuospatial abilities
 346 were significantly and positively associated (red) with residual R_{CT} in clusters within the right superior
 347 parietal cortex, postcentral gyrus, and superior marginal gyrus (mid row). Residual visuospatial abilities
 348 were also negatively correlated with residual R_{CF} within a cluster in the right middle frontal gyrus
 349 (bottom row). The color bar depicts the proportion of explained variance within each cluster in terms of
 350 the determinant of covariation (R^2), overlaid on the inflated cortical surfaces. Scatterplots show
 351 associations of the z-scored, maximal R^2 value of each residual cluster and the respective residual
 352 behavioral test score after removing the effects of age at kindergarten, sex, handedness, non-verbal IQ
 353 at the end of second grade, maternal education, spelling accuracy, reading speed, familial risk of
 354 developing dyslexia, the respective other subscale of the standardized math test, and hemispheric mean
 355 value of investigated morphometric measure at kindergarten age. Shaded areas surrounding regression
 356 lines depict the respective 95% confidence level intervals. All reported results are significant at a level
 357 of $p < 0.05$ (family-wise-error corrected). R_{CT} = relative change rate of cortical thickness; R_{CF} = relative
 358 change rate of cortical folding regularity; MOG = middle occipital gyrus; TP = temporal pole; SMG =
 359 supramarginal gyrus; postCG = postcentral gyrus; SPC = superior parietal cortex; MFG = middle frontal
 360 gyrus.

361 **4. Discussion**

362 In this study, we examined changes in cortical anatomy associated with emerging individual
363 differences in mathematical ability of typically developing children. In contrast to previous
364 studies, we focused on the trajectory from kindergarten to school when children start
365 undergoing formal mathematical education. We correlated the change in various measures of
366 cortical surface morphometry occurring between 5 and 8 years of age with performance on a
367 standardized, age-normed math test. Our analyses revealed a significant negative correlation
368 between change rate of cortical folding regularity and symbolic arithmetic processing in the
369 right IPS. Further, cortical thickness change was negatively correlated with arithmetic
370 performance in the right temporal pole and the left middle occipital gyrus. Moreover, we
371 detected significant positive associations between visuospatial magnitude processing and rate
372 of cortical thickness change of the right superior parietal lobe, right supramarginal gyrus and
373 right postcentral gyrus. Additionally, we found a significant negative correlation between
374 visuospatial magnitude processing score and change of cortical folding regularity of the right
375 MFG.

376 Classical analyses of gray matter volume via voxel-based morphometry cannot disentangle
377 differences driven by cortical thickness and folding regularity (Mechelli et al., 2005). Hence,
378 going beyond volumetric measures, an examination of cortical surface development as provided
379 in our study may give more detailed and specific insights into the intricate relationship between
380 brain maturation and emerging mathematical cognition.

381 Cortical thickness changes may be related to processes affecting the cortical cytoarchitecture,
382 like neuro-, glio- and synaptogenesis as well as synaptic pruning (Zatorre et al., 2012). More
383 recent evidence also suggests that decreases in cortical thickness during development are a
384 marker of progressive growth of deep cortical white matter (Natu et al., 2018). The spatial and

385 temporal progression of these maturational processes follows highly heterogenous patterns
386 throughout the cortex (Huttenlocher and Dabholkar, 1997). Cortical folding during
387 development is driven by physical forces induced by continued growth of outer cortical layers,
388 as neurons form new synaptic connections (Budday et al., 2015b, 2015a). Consequently, the
389 cortical surface expands more quickly than the underlying tissue, creating compression forces
390 that ultimately lead to surface buckling (Richman et al., 1975). Thus, a likely explanation may
391 be that cortical folding changes reflect myelination and synaptic remodeling (Blanton et al.,
392 2001). Nevertheless, future investigations are necessary to validate the neurobiological
393 underpinnings of differential development of cortical surface regularity.

394 Our ROI analysis highlights the link between right IPS folding and mathematical ability.
395 Comparable to our observation for the right MFG, we found a negative association between the
396 change in folding regularity of the right IPS and arithmetic performance. This is in line with
397 the known key role of this region for typical and atypical numerical cognition. Specifically,
398 Cantlon et al. (2006) demonstrate right-lateralized parietal activation related to processing of
399 magnitude in 4-year-old children. **Further, Emerson & Cantlon (2015) identify the right IPS**
400 **as the sole region to continuously exhibit number-selective responses in four- to nine-year-**
401 **old children, emphasizing its developmentally stable involvement in numerical**
402 **processing. This finding is in agreement with reports of age-invariant adaptation effects**
403 **to numerical magnitude across development (Vogel et al., 2015).** Moreover, children and
404 adolescents with low mathematical competence show higher involvement of the right IPS than
405 individuals with high competence when performing simple arithmetic tasks, indicating greater
406 reliance on magnitude processing strategies that rest on basic quantity representations in the
407 parietal cortex (De Smedt et al., 2011; Price et al., 2013). In contrast **to the continuous pattern**
408 **of number-selective responses within the right IPS, number-related neural activity in left**
409 **parietal regions increases from childhood until adolescence (Vogel et al., 2015).**

410 **Longitudinal evidence suggests an association between these left-lateralized age-related**
411 **changes and the refinement of numerical skills in terms of discrimination acuity (Emerson**
412 **and Cantlon, 2015). Further during typical development, the** involvement of left parietal
413 regions **for** symbolic mathematical operations increases **over time** (Rivera et al., 2005),
414 reflecting its functional specialization for memory-based arithmetic processing (Piazza et al.,
415 2007). In the light of these findings, our results suggest that **initial stages of** mathematical
416 learning **are** related to more mature intracortical synaptic connectivity of the right, but not the
417 left, IPS. This process might refine basic magnitude processing strategies, thus strengthening
418 the elementary representations of quantity.

419 Beyond our ROI results, the whole-brain analyses suggest that the rate of neuroplastic change
420 in a region associated with semantic knowledge (Amalric and Dehaene, 2016; Menon, 2015),
421 the right temporal pole, plays an important role for early mathematical development. In
422 particular, cortical thickness change was negatively associated with math performance. The
423 right anterior temporal pole is a multimodal association area known to integrate conceptual
424 information that is distributed across different brain regions (Patterson et al., 2007). In line with
425 this, the children in our study learned first basic mathematical concepts in the period under
426 investigation. Mastering these concepts requires integrating knowledge of number facts,
427 relations between magnitudes and arithmetic principles (Dowker, 2013). Given that, over
428 development, the temporal pole steadily declines in cortical thickness (Ducharme et al., 2016;
429 Fjell et al., 2015), the association between reduced change and high arithmetic performance
430 suggested by our results may indicate a slower trajectory of cortical thinning. This might point
431 to a more sustained build-up of new connections in the right temporal memory system during
432 mathematical learning.

433 The only effect in the left hemisphere obtained from our analyses was a significant negative
434 correlation of cortical thickness change rate and arithmetic abilities within the middle occipital

435 gyrus. Located within the visual association cortex (Brodmann area 18), this region is
436 commonly associated with early stages of visual processing like stereotactic vision (Fortin et
437 al., 2002) and simple pattern recognition (Marcar et al., 2004). Given that mathematical
438 education in school is primarily based on visually presented mathematical problems, this effect
439 might reflect a result of increased visual training specifically related to the visual numerical
440 form. The typical developmental trajectory of such low-level sensory regions follows a linear
441 decrease in thickness (Ducharme et al., 2016), such that the current result may potentially
442 indicate a slower rate of cortical thinning due to this increased visual training in better
443 performing children.

444 The right superior parietal lobe contributes to approximate calculation already in preschool
445 children (Cantlon et al., 2006) and supports exact symbolic calculation in adults (Knops et al.,
446 2009). Our findings complement these data by suggesting a fundamental contribution of
447 superior parietal lobe plasticity for the transition from approximate to exact calculation by
448 refining visuospatial magnitude processing skills. Within the age range under investigation
449 here, cortical thickness increases in parietal regions before subsequently declining later in life
450 (Ducharme et al., 2016; Shaw et al., 2008). The positive association between thickness change
451 and mathematical ability might therefore suggest that increased synaptogenesis supports
452 mathematical learning in the first school years.

453 Cytoarchitectonic subdivisions of the right supramarginal gyrus have been shown to exhibit
454 heterogenous patterns of activation across development of arithmetic problem solving skills
455 from primary school-age until adulthood (Chang et al., 2016). Our findings add to these results,
456 pointing towards a positive association between cortical thickness change and visuo-spatial
457 magnitude processing already at the transition between kindergarten and second grade in
458 school. Supramarginal cortical thickness typically decreases following a linear trajectory from
459 childhood until adulthood (Ducharme et al., 2016). Thus, the clusters detected in the current

460 analysis likely point towards accelerated cortical thickness change potentially driven by
461 increases in cortical white matter, supporting the development of visuo-spatial magnitude
462 processing abilities. It is noteworthy, however, that these associations were not revealed in our
463 ROI analyses but only in the whole brain contrast. A reason for this discrepancy may be that
464 we choose a rather large ROI combining SMG subregions PFop, PF, and PFm, while the whole
465 brain analysis revealed two confined clusters partly located in PF. Thus, computing the mean
466 cortical folding regularity across this combined region possibly concealed the relationship
467 between behavior and cortical change indeed present in its subcomponents.

468 Somewhat unexpected, our analyses additionally revealed a positive association between
469 visuospatial processing skills and cortical thickness change of the right lateral postcentral gyrus.
470 This region is associated with cortical thinning over development (Ducharme et al., 2016).
471 While the exact role of this region for numerical cognition is still elusive, there is evidence that
472 functional connectivity between the right postcentral gyrus and the left angular gyrus, a key
473 region associated with verbal mathematical fact retrieval, significantly increases after intensive
474 math tutoring in children (Jolles et al., 2016b). Further, it is the locus of somatosensory regions
475 that have been suggested to impact the allocation of attention in visual space (Balslev et al.,
476 2013). In line with this, our findings suggest a link between visuospatial processing ability and
477 more rapid growth of cortical white matter indicated by increased rates of cortical thinning.

478 Further, our results show that better visuospatial performance was negatively associated with
479 change in the regularity of cortical folding within the right MFG, a region consistently activated
480 in calculation tasks with higher working memory demands (Menon, 2000). Changes in the
481 regularity of cortical folding are assumed to be linked to the persistent growth of superficial
482 cortical layers driven by the formation of new intracortical synaptic connections (Budday et al.,
483 2015b, 2015a). Children with higher mathematical ability might thus exhibit more mature
484 intracortical synaptic connectivity in the right MFG.

485 In a recent study, Nemmi et al. (2018) demonstrated that the right number-form area shows
486 specific functional connectivity to the right IPS already at three years of age. Differential
487 connectivity to parietal and prefrontal regions associated with gains in mathematical ability,
488 however, emerged only later around 12–14 years of age. In line with this tentative
489 developmental trajectory, our analyses did not reveal associations between mathematical
490 abilities and surface plasticity of the VTOC from kindergarten to second grade in school. Future
491 studies are needed to examine the relationship between structural changes of this region and
492 mathematical ability in older children who encounter more challenging mathematical concepts
493 in higher grades.

494 Despite providing insights into associations between cortical surface plasticity and individual
495 behavioural performance, it is impossible to derive definite conclusions about the exact role of
496 localized cortical changes for cognitive functioning from the current data. For instance, the
497 parietal cortex including the IPS is known to be involved in a multitude of different cognitive
498 mechanisms beyond core mathematical processing, including non-spatial working memory
499 and executive functioning (see Culham and Kanwisher, 2001 for a review). Even within the
500 domain of magnitude processing, animal work suggests distinct neural processing stages
501 within this region (Nieder et al., 2006). Thus, it is not clear which aspects involved in the
502 complex cognitive functions investigated here the observed changes support. Still, our
503 results guide the formation of hypotheses for future longitudinal work disentangling these
504 specific contributions of individual areas to mathematical cognition.

505 A number of methodological limitations have to be considered. First, it is important to stress
506 that the results presented here are correlational. Consequently, the current analysis cannot
507 disentangle the extent to which brain maturational processes induce changes in individual
508 abilities from the extent to which mathematical and visuo-spatial training re-shapes the cortical
509 structure. Second, considering the known importance of the ROIs under investigation for

510 mathematical processing, the null results reported here need to be interpreted with caution.
511 Third, the scanner upgrade between time point 1 and time point 2 might bias findings if there
512 is an interaction between upgrade and an individual factor which correlated with math skill
513 development. **Fourth, our selection of atlas ROIs was based on insights from single**
514 **studies and thus might be prone to individual variance, given the lack of an appropriate**
515 **meta-analysis quantifying functional development of arithmetic and visuospatial**
516 **magnitude processing in children from kindergarten to second grade in school.** Last,
517 given the limited sample size, spatial detection of relatively small significant clusters as
518 reported here might be sensitive to subtle methodological variations. Hence, the results from
519 this work await confirmation in larger follow-up studies.

520 In conclusion, the present study provides evidence that cortical surface morphometry changes
521 are linked to mathematical learning during the first years of formal instruction. A series of
522 whole brain analyses highlights the importance of regions associated with working memory
523 and semantic memory processes, such as the right middle frontal gyrus, the right precentral
524 gyrus, and the right temporal pole. Furthermore, our results emphasize the role of surface
525 reorganization within the right superior parietal lobe, supporting visuospatial processing, and
526 within the right intraparietal sulcus as a crucial area for numerical magnitude processing. Thus,
527 we identify early cortical surface plasticity as an important structural correlate of emerging
528 arithmetic abilities during the first years of school.

529 **Acknowledgements:** This work was supported by the Max Planck Society and the Fraunhofer
530 Society (grant number M.FE.A.NEPF0001). We would like to thank all members of the
531 LEGASCREEN consortium for their support during this study.

532 **References**

- 533 Amalric, M., Dehaene, S., 2016. Origins of the brain networks for advanced mathematics in expert
534 mathematicians. *Proc. Natl. Acad. Sci. U. S. A.* 113, 4909–4917.
535 <https://doi.org/10.1073/pnas.1603205113>
- 536 Avants, B.B., Tustison, N.J., Song, G., Cook, P.A., Klein, A., Gee, J.C., 2011. A reproducible
537 evaluation of ANTs similarity metric performance in brain image registration. *NeuroImage*
538 54, 2033–2044. <https://doi.org/10.1016/j.neuroimage.2010.09.025>
- 539 Avants, B.B., Yushkevich, P., Pluta, J., Minkoff, D., Korczykowski, M., Detre, J., Gee, J.C., 2010.
540 The optimal template effect in hippocampus studies of diseased populations. *NeuroImage* 49,
541 2457–2466. <https://doi.org/10.1016/j.neuroimage.2009.09.062>
- 542 Balslev, D., Odoj, B., Karnath, H.-O., 2013. Role of Somatosensory Cortex in Visuospatial Attention.
543 *J. Neurosci.* 33, 18311–18318. <https://doi.org/10.1523/JNEUROSCI.1112-13.2013>
- 544 Barth, H., La Mont, K., Lipton, J., Spelke, E.S., 2005. Abstract number and arithmetic in preschool
545 children. *Proc. Natl. Acad. Sci. U. S. A.* 102, 14116–14121.
546 <https://doi.org/10.1073/pnas.0505512102>
- 547 Barth, H., La Mont, K., Lipton, J.S., Dehaene, S., Kanwisher, N., Spelke, E.S., 2006. Non-symbolic
548 arithmetic in adults and young children. *Cognition* 98, 199–222.
- 549 Blanton, R.E., Levitt, J.G., Thompson, P.M., Narr, K.L., Capetillo-Cunliffe, L., Nobel, A., Singerman,
550 J.D., McCracken, J.T., Toga, A.W., 2001. Mapping cortical asymmetry and complexity
551 patterns in normal children. *Psychiatry Res. Neuroimaging* 107, 29–43.
552 [https://doi.org/10.1016/S0925-4927\(01\)00091-9](https://doi.org/10.1016/S0925-4927(01)00091-9)
- 553 Brown, M., Askew, M., Rhodes, V., Denvir, H., Ranson, E., Wiliam, D., 2003. Characterising
554 individual and cohort progression in learning numeracy: results from the Leverhulme 5-year

555 longitudinal study. Presented at the American Educational Research Association Annual
556 Conference, Chicago, pp. 21–25.

557 Budday, S., Steinmann, P., Kuhl, E., 2015a. Physical biology of human brain development. *Front.*
558 *Cell. Neurosci.* 9, 257. <https://doi.org/10.3389/fncel.2015.00257>

559 Budday, S., Steinmann, P., Kuhl, E., 2015b. Secondary instabilities modulate cortical complexity in
560 the mammalian brain. *Philos. Mag.* 95, 3244–3256.
561 <https://doi.org/10.1080/14786435.2015.1024184>

562 Bull, R., Espy, K.A., Wiebe, S.A., 2008. Short-Term Memory, Working Memory, and Executive
563 Functioning in Preschoolers: Longitudinal Predictors of Mathematical Achievement at Age 7
564 Years. *Dev. Neuropsychol.* 33, 205–228. <https://doi.org/10.1080/87565640801982312>

565 Bullmore, E., Sporns, O., 2012. The economy of brain network organization. *Nat. Rev. Neurosci.* 13,
566 336–349. <https://doi.org/10.1038/nrn3214>

567 Cafiero, R., Brauer, J., Anwander, A., Friederici, A.D., 2018. The concurrence of cortical surface area
568 expansion and white matter myelination in human brain development. *Cereb. Cortex* 29, 827–
569 837. <https://doi.org/10.1093/cercor/bhy277>

570 Cantlon, J.F., Brannon, E.M., Carter, E.J., Pelphey, K.A., 2006. Functional imaging of numerical
571 processing in adults and 4-y-old children. *PLOS Biol.* 4, e125.
572 <https://doi.org/10.1371/journal.pbio.0040125>

573 Chang, T.-T., Metcalfe, A.W.S., Padmanabhan, A., Chen, T., Menon, V., 2016. Heterogeneous and
574 nonlinear development of human posterior parietal cortex function. *NeuroImage* 126, 184–
575 195. <https://doi.org/10.1016/j.neuroimage.2015.11.053>

576 Cho, S., Ryali, S., Geary, D.C., Menon, V., 2011. How does a child solve $7 + 8$? Decoding brain
577 activity patterns associated with counting and retrieval strategies. *Dev. Sci.* 14, 989–1001.
578 <https://doi.org/10.1111/j.1467-7687.2011.01055.x>

- 579 Cockcroft, W.H., 1982. Mathematics counts. HM Stationery Office, London.
- 580 Culham, J.C., Kanwisher, N.G., 2001. Neuroimaging of cognitive functions in human parietal cortex.
581 *Curr. Opin. Neurobiol.* 11, 157–163. [https://doi.org/10.1016/S0959-4388\(00\)00191-4](https://doi.org/10.1016/S0959-4388(00)00191-4)
- 582 De Smedt, B., Holloway, I.D., Ansari, D., 2011. Effects of problem size and arithmetic operation on
583 brain activation during calculation in children with varying levels of arithmetical fluency.
584 *NeuroImage, Special Issue: Educational Neuroscience* 57, 771–781.
585 <https://doi.org/10.1016/j.neuroimage.2010.12.037>
- 586 De Smedt, B., Janssen, R., Bouwens, K., Verschaffel, L., Boets, B., Ghesquière, P., 2009. Working
587 memory and individual differences in mathematics achievement: A longitudinal study from
588 first grade to second grade. *J. Exp. Child Psychol.* 103, 186–201.
589 <https://doi.org/10.1016/j.jecp.2009.01.004>
- 590 Dehaene, S., 2011. The number sense: How the mind creates mathematics, revised and updated
591 edition. Oxford University Press, USA.
- 592 Dirks, E., Spyer, G., van Lieshout, E.C.D.M., de Sonneville, L., 2008. Prevalence of combined
593 reading and arithmetic disabilities. *J. Learn. Disabil.* 41, 460–473.
594 <https://doi.org/10.1177/0022219408321128>
- 595 Dowker, A., 2013. Individual differences in arithmetical abilities. Psychology Press, New York, NY,
596 US.
- 597 Ducharme, S., Albaugh, M.D., Nguyen, T.-V., Hudziak, J.J., Mateos-Pérez, J.M., Labbe, A., Evans,
598 A.C., Karama, S., 2016. Trajectories of cortical thickness maturation in normal brain
599 development — The importance of quality control procedures. *NeuroImage* 125, 267–279.
600 <https://doi.org/10.1016/j.neuroimage.2015.10.010>
- 601 Duncan, G.J., Dowsett, C.J., Claessens, A., Magnuson, K., Huston, A.C., Klebanov, P., Pagani, L.S.,
602 Feinstein, L., Engel, M., Brooks-Gunn, J., Sexton, H., Duckworth, K., Japel, C., 2007. School

603 readiness and later achievement. *Dev. Psychol.* 43, 1428–1446. <https://doi.org/10.1037/0012->
604 1649.43.6.1428

605 Emerson, R.W., Cantlon, J.F., 2015. Continuity and change in children’s longitudinal neural responses
606 to numbers. *Dev. Sci.* 18, 314–326. <https://doi.org/10.1111/desc.12215>

607 Evans, T.M., Kochalka, J., Ngoon, T.J., Wu, S.S., Qin, S., Battista, C., Menon, V., 2015. Brain
608 structural integrity and intrinsic functional connectivity forecast 6 year longitudinal growth in
609 children’s numerical abilities. *J. Neurosci.* 35, 11743–11750.
610 <https://doi.org/10.1523/JNEUROSCI.0216-15.2015>

611 Fjell, A.M., Grydeland, H., Krogstad, S.K., Amlie, I., Rohani, D.A., Ferschmann, L., Storsve, A.B.,
612 Tamnes, C.K., Sala-Llloch, R., Due-Tønnessen, P., Bjørnerud, A., Sølvsnes, A.E., Håberg,
613 A.K., Skranes, J., Bartsch, H., Chen, C.-H., Thompson, W.K., Panizzon, M.S., Kremen, W.S.,
614 Dale, A.M., Walhovd, K.B., 2015. Development and aging of cortical thickness correspond to
615 genetic organization patterns. *Proc. Natl. Acad. Sci. U. S. A.* 112, 15462–15467.
616 <https://doi.org/10.1073/pnas.1508831112>

617 Fonov, V.S., Evans, A.C., McKinstry, R.C., Almlie, C.R., Collins, D.L., 2009. Unbiased nonlinear
618 average age-appropriate brain templates from birth to adulthood. *NeuroImage Supplement* 1,
619 S102. [https://doi.org/10.1016/S1053-8119\(09\)70884-5](https://doi.org/10.1016/S1053-8119(09)70884-5)

620 Formisano, E., Linden, D.E.J., Di Salle, F., Trojano, L., Esposito, F., Sack, A.T., Grossi, D., Zanella,
621 F.E., Goebel, R., 2002. Tracking the Mind’s Image in the Brain I: Time-Resolved fMRI
622 during Visuospatial Mental Imagery. *Neuron* 35, 185–194. <https://doi.org/10.1016/S0896->
623 6273(02)00747-X

624 Fortin, A., Ptito, A., Faubert, J., Ptito, M., 2002. Cortical areas mediating stereopsis in the human
625 brain: a PET study. *Neuroreport* 13, 895–898.

- 626 Georges, C., Hoffmann, D., Schiltz, C., 2017. Mathematical abilities in elementary school: Do they
627 relate to number–space associations? *J. Exp. Child Psychol.* 161, 126–147.
628 <https://doi.org/10.1016/j.jecp.2017.04.011>
- 629 Glasser, M.F., Coalson, T.S., Robinson, E.C., Hacker, C.D., Harwell, J., Yacoub, E., Ugurbil, K.,
630 Andersson, J.L.R., Beckmann, C.F., Jenkinson, M., Smith, S.M., Van Essen, D.C., 2016. A
631 multi-modal parcellation of human cerebral cortex. *Nature* 536, 171–178.
632 <https://doi.org/10.1038/nature18933>
- 633 Grabner, R.H., Ansari, D., Reishofer, G., Stern, E., Ebner, F., Neuper, C., 2007. Individual differences
634 in mathematical competence predict parietal brain activation during mental calculation.
635 *NeuroImage* 38, 346–356. <https://doi.org/10.1016/j.neuroimage.2007.07.041>
- 636 Haffner, J., Baro, K., Parzer, P., Resch, F., 2005. Heidelberger Rechentest (HRT 1-4). Hogrefe,
637 Göttingen.
- 638 Hannagan, T., Amedi, A., Cohen, L., Dehaene-Lambertz, G., Dehaene, S., 2015. Origins of the
639 specialization for letters and numbers in ventral occipitotemporal cortex. *Trends Cogn. Sci.*
640 19, 374–382. <https://doi.org/10.1016/j.tics.2015.05.006>
- 641 He, L., Zuo, Z., Chen, L., Humphreys, G., 2014. Effects of Number Magnitude and Notation at 7T:
642 Separating the Neural Response to Small and Large, Symbolic and Nonsymbolic Number.
643 *Cereb. Cortex* 24, 2199–2209. <https://doi.org/10.1093/cercor/bht074>
- 644 Holm, S., 1979. A Simple Sequentially Rejective Multiple Test Procedure. *Scand. J. Stat.* 6, 65–70.
- 645 Huttenlocher, P.R., Dabholkar, A.S., 1997. Regional differences in synaptogenesis in human cerebral
646 cortex. *J. Comp. Neurol.* 387, 167–178. [https://doi.org/10.1002/\(SICI\)1096-
647 9861\(19971020\)387:2<167::AID-CNE1>3.0.CO;2-Z](https://doi.org/10.1002/(SICI)1096-9861(19971020)387:2<167::AID-CNE1>3.0.CO;2-Z)
- 648 Jolles, D., Ashkenazi, S., Kochalka, J., Evans, T.M., Richardson, J., Rosenberg-Lee, M., Zhao, H.,
649 Supekar, K., Chen, T., Menon, V., 2016a. Parietal hyper-connectivity, aberrant brain

650 organization, and circuit- based biomarkers in children with mathematical disabilities. *Dev.*
651 *Sci.* 19, 613–631. <https://doi.org/10.1111/desc.12399>

652 Jolles, D., Supekar, K., Richardson, J., Tenison, C., Ashkenazi, S., Rosenberg-Lee, M., Fuchs, L.,
653 Menon, V., 2016b. Reconfiguration of parietal circuits with cognitive tutoring in elementary
654 school children. *Cortex* 83, 231–245. <https://doi.org/10.1016/j.cortex.2016.08.004>

655 Klingberg, T., Forssberg, H., Westerberg, H., 2002. Increased Brain Activity in Frontal and Parietal
656 Cortex Underlies the Development of Visuospatial Working Memory Capacity during
657 Childhood. *J. Cogn. Neurosci.* 14, 1–10. <https://doi.org/10.1162/089892902317205276>

658 Knops, A., Thirion, B., Hubbard, E.M., Michel, V., Dehaene, S., 2009. Recruitment of an area
659 involved in eye movements during mental arithmetic. *Science* 324, 1583–1585.
660 <https://doi.org/10.1126/science.1171599>

661 Kwon, H., Reiss, A.L., Menon, V., 2002. Neural basis of protracted developmental changes in visuo-
662 spatial working memory. *Proc. Natl. Acad. Sci.* 99, 13336–13341.
663 <https://doi.org/10.1073/pnas.162486399>

664 Lipton, J.S., Spelke, E.S., 2003. Origins of number sense: Large-number discrimination in human
665 infants. *Cognition* 14, 396–401.

666 Lüders, E., Thompson, P.M., Narr, K.L., Toga, A.W., Jäncke, L., Gaser, C., 2006. A curvature-based
667 approach to estimate local gyrification on the cortical surface. *NeuroImage* 29, 1224–1230.
668 <https://doi.org/10.1016/j.neuroimage.2005.08.049>

669 Marcar, V.L., Loenneker, T., Straessle, A., Jaggy, S., Kucian, K., Martin, E., 2004. An fMRI study of
670 the cerebral macro network involved in “cue invariant” form perception and how it is
671 influenced by stimulus complexity. *NeuroImage* 23, 947–955.
672 <https://doi.org/10.1016/j.neuroimage.2004.05.028>

673 Masataka, N., Ohnishi, T., Imabayashi, E., Hirakata, M., Matsuda, H., 2007. Neural correlates for
674 learning to read Roman numerals. *Brain Lang.* 100, 276–282.
675 <https://doi.org/10.1016/j.bandl.2006.11.011>

676 Mechelli, A., Price, C.J., Friston, K.J., Ashburner, J.T., 2005. Voxel-based morphometry of the human
677 brain: Methods and applications. *Curr. Med. Imaging Rev.* 1, 105–113.
678 <https://doi.org/10.2174/1573405054038726>

679 Menon, V., 2015. Arithmetic in the child and adult brain, in: Kadosh, R.C., Dowker, A. (Eds.), *The*
680 *Oxford Handbook of Numerical Cognition*, Oxford Library of Psychology. Oxford University
681 Press, New York, NY, US, pp. 502–530.

682 Menon, V., 2010. Developmental cognitive neuroscience of arithmetic: Implications for learning and
683 education. *ZDM Int. J. Math. Educ.* 42, 515–525. <https://doi.org/10.1007/s11858-010-0242-0>

684 Menon, V., Rivera, S.M., White, C.D., Glover, G.H., Reiss, A.L., 2000. Dissociating prefrontal and
685 parietal cortex activation during arithmetic processing. *NeuroImage* 12, 357–365.
686 <https://doi.org/10.1006/nimg.2000.0613>

687 Moll, K., Kunze, S., Neuhoff, N., Bruder, J., Schulte-Körne, G., 2014. Specific learning disorder:
688 Prevalence and gender differences. *PLOS ONE* 9, e103537.
689 <https://doi.org/10.1371/journal.pone.0103537>

690 Moll, K., Landerl, K., 2010. *SLRT-II: Lese- und Rechtschreibtest; Weiterentwicklung des Salzburger*
691 *Lese- und Rechtschreibtests (SLRT)*. Hans Huber, Bern.

692 Natu, V.S., Gomez, J., Barnett, M., Jeska, B., Kirilina, E., Jaeger, C., Zhen, Z., Cox, S., Weiner, K.S.,
693 Weiskopf, N., Grill-Spector, K., 2018. Apparent thinning of visual cortex during childhood is
694 associated with myelination, not pruning. *bioRxiv* 368274. <https://doi.org/10.1101/368274>

695 Nemmi, F., Schel, M.A., Klingberg, T., 2018. Connectivity of the human number form area reveals
696 development of a cortical network for mathematics. *Front. Hum. Neurosci.* 12.
697 <https://doi.org/10.3389/fnhum.2018.00465>

698 Nieder, A., Diester, I., Tudusciuc, O., 2006. Temporal and spatial enumeration processes in the
699 primate parietal cortex 313, 6.

700 Oldfield, R.C., 1971. The assessment and analysis of handedness: The Edinburgh inventory.
701 *Neuropsychologia* 9, 97–113. [https://doi.org/10.1016/0028-3932\(71\)90067-4](https://doi.org/10.1016/0028-3932(71)90067-4)

702 Patterson, K., Nestor, P.J., Rogers, T.T., 2007. Where do you know what you know? The
703 representation of semantic knowledge in the human brain. *Nat. Rev. Neurosci.* 8, 976–987.
704 <https://doi.org/10.1038/nrn2277>

705 Petermann, F., Petermann, U., 2011. Wechsler Intelligence Scale for Children: Fourth Edition (WISC-
706 IV). German Version. Pearson Assessment, Frankfurt am Main.

707 Peters, L., De Smedt, B., 2018. Arithmetic in the developing brain: A review of brain imaging studies.
708 *Dev. Cogn. Neurosci.* 30, 265–279. <https://doi.org/10.1016/j.dcn.2017.05.002>

709 Peters, L., Polspoel, B., Op de Beeck, H., De Smedt, B., 2016. Brain activity during arithmetic in
710 symbolic and non-symbolic formats in 9–12 year old children. *Neuropsychologia* 86, 19–28.
711 <https://doi.org/10.1016/j.neuropsychologia.2016.04.001>

712 Piazza, M., Izard, V., Pinel, P., Le Bihan, D., Dehaene, S., 2004. Tuning curves for approximate
713 numerosity in the human intraparietal sulcus. *Neuron* 44, 547–555.
714 <https://doi.org/10.1016/j.neuron.2004.10.014>

715 Piazza, M., Mechelli, A., Price, C.J., Butterworth, B., 2006. Exact and approximate judgements of
716 visual and auditory numerosity: An fMRI study. *Brain Res.* 1106, 177–188.

717 Piazza, M., Pinel, P., Le Bihan, D., Dehaene, S., 2007. A magnitude code common to numerosities
718 and number symbols in human intraparietal cortex. *Neuron* 53, 293–305.
719 <https://doi.org/10.1016/j.neuron.2006.11.022>

720 Price, G.R., Mazzocco, M.M.M., Ansari, D., 2013. Why Mental Arithmetic Counts: Brain Activation
721 during Single Digit Arithmetic Predicts High School Math Scores. *J. Neurosci.* 33, 156–163.
722 <https://doi.org/10.1523/JNEUROSCI.2936-12.2013>

723 Qin, S., Cho, S., Chen, T., Rosenberg-Lee, M., Geary, D.C., Menon, V., 2014. Hippocampal-
724 neocortical functional reorganization underlies children’s cognitive development. *Nat.*
725 *Neurosci.* 17, 1263–1269. <https://doi.org/10.1038/nn.3788>

726 R Core Team, 2016. R: A language and environment for statistical computing. R Foundation for
727 Statistical Computing, Vienna, Austria.

728 Rasmussen, C., Bisanz, J., 2005. Representation and working memory in early arithmetic. *J. Exp.*
729 *Child Psychol.* 91, 137–157. <https://doi.org/10.1016/j.jecp.2005.01.004>

730 Raznahan, A., Shaw, P., Lalonde, F., Stockman, M., Wallace, G.L., Greenstein, D., Clasen, L.,
731 Gogtay, N., Giedd, J.N., 2011. How Does Your Cortex Grow? *J. Neurosci. Off. J. Soc.*
732 *Neurosci.* 31, 7174–7177. <https://doi.org/10.1523/JNEUROSCI.0054-11.2011>

733 Richman, D.P., Stewart, R.M., Hutchinson, J.W., Caviness, V.S., Jr, 1975. Mechanical model of brain
734 convolitional development. *Science* 189, 18–21.

735 Rivera, S.M., Reiss, A.L., Eckert, M.A., Menon, V., 2005. Developmental changes in mental
736 arithmetic: Evidence for increased functional specialization in the left inferior parietal cortex.
737 *Cereb. Cortex* 15, 1779–1790. <https://doi.org/10.1093/cercor/bhi055>

738 Schel, M.A., Klingberg, T., 2017. Specialization of the right intraparietal sulcus for processing
739 mathematics during development. *Cereb. Cortex* 27, 4436–4446.
740 <https://doi.org/10.1093/cercor/bhw246>

741 Schnack, H.G., van Haren, N.E.M., Brouwer, R.M., Evans, A., Durston, S., Boomsma, D.I., Kahn,
742 R.S., Hulshoff Pol, H.E., 2015. Changes in Thickness and Surface Area of the Human Cortex
743 and Their Relationship with Intelligence. *Cereb. Cortex* 25, 1608–1617.
744 <https://doi.org/10.1093/cercor/bht357>

745 Shaw, P., Kabani, N.J., Lerch, J.P., Eckstrand, K., Lenroot, R.K., Gogtay, N., Greenstein, D., Clasen,
746 L., Evans, A.C., Rapoport, J.L., Giedd, J.N., Wise, S.P., 2008. Neurodevelopmental
747 trajectories of the human cerebral cortex. *J. Neurosci.* 28, 3586–3594.
748 <https://doi.org/10.1523/JNEUROSCI.5309-07.2008>

749 Slaughter, V., Kamppi, D., Paynter, J., 2006. Toddler subtraction with large sets: further evidence for
750 an analog-magnitude representation of number. *Dev. Sci.* 9, 33–39.
751 <https://doi.org/10.1111/j.1467-7687.2005.00460.x>

752 Stock, C., Schneider, W., 2008. DERET 1–2+: Deutscher Rechtschreibtest für das erste und zweite
753 Schuljahr. Hogrefe, Göttingen.

754 Supekar, K., Swigart, A.G., Tenison, C., Jolles, D.D., Rosenberg-Lee, M., Fuchs, L., Menon, V.,
755 2013. Neural predictors of individual differences in response to math tutoring in primary-
756 grade school children. *Proc. Natl. Acad. Sci. U. S. A.* 110, 8230–8235.
757 <https://doi.org/10.1073/pnas.1222154110>

758 Venkatraman, V., Ansari, D., Chee, M.W.L., 2005. Neural correlates of symbolic and non-symbolic
759 arithmetic. *Neuropsychologia* 43, 744–753.
760 <https://doi.org/10.1016/j.neuropsychologia.2004.08.005>

761 Vogel, S.E., Goffin, C., Ansari, D., 2015. Developmental specialization of the left parietal cortex for
762 the semantic representation of Arabic numerals: An fMR-adaptation study. *Dev. Cogn.*
763 *Neurosci.* 12, 61–73. <https://doi.org/10.1016/j.dcn.2014.12.001>

764 Wechsler, D., Petermann, F., Lipsius, M., 2009. WPPSI-III: Wechsler preschool and primary scale of
765 intelligence. German Version. Pearson Assessment, Frankfurt am Main.

766 Xu, F., Spelke, E.S., 2000. Large number discrimination in 6-month-old infants. *Cognition* 74, B1–
767 B11.

768 Yeo, D.J., Wilkey, E.D., Price, G.R., 2017. The search for the number form area: A functional
769 neuroimaging meta-analysis. *Neurosci. Biobehav. Rev.* 78, 145–160.
770 <https://doi.org/10.1016/j.neubiorev.2017.04.027>

771 Yotter, R.A., Nenadic, I., Ziegler, G., Thompson, P.M., Gaser, C., 2011. Local cortical surface
772 complexity maps from spherical harmonic reconstructions. *NeuroImage* 56, 961–973.
773 <https://doi.org/10.1016/j.neuroimage.2011.02.007>

774 Zatorre, R.J., Fields, R.D., Johansen-Berg, H., 2012. Plasticity in gray and white: neuroimaging
775 changes in brain structure during learning. *Nat. Neurosci.* 15, 528–536.
776 <https://doi.org/10.1038/nn.3045>

777 Zhang, Y., Brady, M., Smith, S.M., 2001. Segmentation of brain MR images through a hidden Markov
778 random field model and the expectation-maximization algorithm. *IEEE Trans. Med. Imaging*
779 20, 45–57. <https://doi.org/10.1109/42.906424>

780

781 **Declarations of interest:** none

782

783 **Author contributions:** UK, ADF and MAS designed the study. MAS collected the data. UK
784 and MAS analyzed the data. All authors interpreted the data. UK wrote the manuscript. All
785 authors critically reviewed and approved the manuscript.

786

787 **Data and code availability:** The data and/or code used in the current study are available from
788 the corresponding author upon reasonable request.

789

790 **Members of the LEGASCREEN consortium:** The LEGASCREEN consortium comprises
791 the Max Planck Institute for Human Cognitive and Brain Sciences and the Fraunhofer
792 Institute for Cell Therapy and Immunology. The consortium consists of: Prof. Dr. Dr. h.c.
793 Angela D. Friederici, Prof. Dr. Frank Emmrich, Dr. Jens Brauer, Dr. Arndt Wilcke, Dr.
794 Nicole Neef, Prof. Dr. Dr. Johannes Boltze, Dr. Michael Skeide, Dr. Holger Kirsten, Dr. Gesa
795 Schaadt, Dr. Bent Müller, Dr. Indra Kraft, Ivonne Czepezauer, and Liane Dörr.

796

797 **Supplementary materials**

798

799 **Supplementary Table S1. Definition of cortical regions of interest.**

| Regions of interest | Atlas labels^a |
|---|---|
| left / right intraparietal sulcus (IPS) | L_IPS1_ROI, L_MIP_ROI /, R_IPS1_ROI, R_MIP_ROI |
| left / right supramarginal gyrus (SMG) | L_PFop_ROI, L_PF_ROI, L_PFm_ROI / R_PFop_ROI, R_PF_ROI, R_PFm_ROI / |
| Left / right angular gyrus (AG) | L_PGp_ROI, L_PGi_ROI, L_PGs_ROI / R_PGp_ROI, R_PGi_ROI, R_PGs_ROI / |
| left / right hippocampus | L_H_ROI / R_H_ROI |
| left / right dorso-lateral prefrontal cortex (DLPFC) | L_9p_ROI, L_p9-46v_ROI, L_46_ROI, L_a9-46v_ROI, L_9-46d_ROI, L_9a_ROI / R_9p_ROI, R_p9-46v_ROI, R_46_ROI, R_a9-46v_ROI, R_9-46d_ROI, R_9a_ROI |
| left / right ventral temporal-occipital cortex (VTOC) | L_TE1p_ROI / R_TE1p_ROI |
| left / right visual word form area (VWFA) | L_VVC_ROI / R_VVC_ROI |

800 BA=Brodmann area; ^a Glasser et al. (2016), *retrieved 09/01/2016 from <https://balsa.wustl.edu/study/show/RVVG>*; if several areas are given,

801 they were combined to form the final region of interest.

802

803 **Supplementary Table S2. Correlations between covariates for time point 1.** Note that
 804 none of the correlations reaches significance after adjusting for multiple comparisons with
 805 alpha = 0.05.
 806

| | Sex | Handedness | Maternal education | Familial risk of developmental dyslexia | IQ at time point 1 |
|--|------------------------|-----------------------|---------------------------|--|---------------------------|
| Age at time point 1 | r= -0.36; p= 0.0555 | r= 0.13; p=0.5050 | r= 0.06; p=0.7755 | R= -0.16; p=0.4274 | r= -0.05; p=0.7985 |
| Sex | | r= -0.05; p=0.8133 | r= -0.02; p=0.9066 | r= 0.13; p=0.5200 | r= -0.13; p=0.4988 |
| Handedness | | | r= -0.14; p=0.4906 | r= -0.02; p=0.9190 | r= 0.00; p=0.9986 |
| Maternal education | | | | r= 0.29; p=0.1310 | r= 0.36; p=0.0622 |
| Familial risk of developmental dyslexia | | | | | r= 0.32; p=0.0957 |

807

808 **Supplementary Table S3. Correlations between covariates for time point 2.** Note that
 809 none of the correlations reaches significance after adjusting for multiple comparisons with
 810 alpha = 0.05.
 811

| | Sex | Handed- ness | Maternal education | Familial risk of dyslexia | IQ at time point 2 | Spelling accuracy | Reading speed | Arithme- tic abilities | Visuo- spatial abilities |
|--|----------------------|-------------------------|-------------------------------|--|-----------------------------------|------------------------------|--------------------------|---------------------------------------|---|
| Age at time point 2 | r=-0.13 p= 0.5246 | r=0.14; p= 0.4624 | r=0.14; p= 0.4806 | r=-0.38; p= 0.0476 | r= 0.10; p= 0.6097 | r=-0.24; p= 0.2279 | r=0.16 p= 0.4089 | r=-0.27; p= 0.1581 | r=0.05 p= 0.8159 |
| Sex | | r= -0.05; p=0.8133 | r= -0.02; p=0.9066 | r= 0.13; p=0.5200 | r= 0.18; p=0.3566 | r= 0.02; p=0.9263 | r= -0.43; p=0.0208 | r= -0.18; p=0.3555 | r= -0.02; p=0.9348 |
| Handed- ness | | | r= -0.14; p=0.4906 | r= -0.02; p=0.9190 | r= 0.17; p=0.3984 | r= -0.15; p=0.4333 | r= 0.06; p=0.7797 | r= 0.30; p=0.1224 | r= 0.07; p=0.7287 |
| Maternal education | | | | r= 0.29; p=0.1310 | r= 0.27; p=0.1673 | r= 0.16; p=0.4164 | r= 0.26; p=0.1878 | r= 0.23; p=0.2448 | r= 0.51; p=0.0057 |
| Familial risk of dyslexia | | | | | r= 0.23; p=0.2463 | r= 0.01; p=0.9691 | r= -0.28; p=0.1470 | r= 0.39; p=0.0424 | r= 0.55; p=0.0023 |
| IQ at time point 2 | | | | | | r= -0.14; p=0.4892 | r= -0.11; p=0.5911 | r= 0.17; p=0.3930 | r= 0.24; p=0.2254 |
| Spelling accuracy | | | | | | | r= 0.31; p=0.1114 | r= 0.47; p=0.0114 | r= 0.19; p=0.3264 |
| Reading speed | | | | | | | | r= 0.25; p=0.1926 | r= 0.23; p=0.2422 |
| Arithme- tic abilities | | | | | | | | | r= 0.55; p=0.0023 |

812
 813

814 **Supplementary Table S4. Correlations across time.** Significant correlations (alpha < 0.05)
 815 are marked in bold font and with *.
 816

| | Age at time point 2 | | IQ at time point2 |
|--------------------------------|--------------------------------|-------------------|------------------------------|
| Age at time point 1 | r= 0.51; p= 0.0054* | IQ at time point1 | r= 0.33; p= 0.0827 |

817

818 **Supplementary Table S5. Results of the ROI analyses.** Significant effects are marked in
819 italic and bold. To control for multiple comparisons, only results with a $p < 0.0018$ (corrected
820 for 14 ROIs and 2 math test subscales) are considered significant. TE1p = VTOC

| | Arithmetic abilities | | Visuo-spatial abilities | | | Arithmetic abilities | | Visuo-spatial abilities | |
|------------------------------|----------------------|--------|-------------------------|--------|---------------------|----------------------|----------------------|-------------------------|--------|
| | R ² | P | R ² | P | | R ² | P | R ² | P |
| <i>R_{CT}</i> | | | | | | | | | |
| L IPS | 0.06 | 0.3273 | 0.01 | 0.6751 | R IPS | 0.00 | 0.9574 | 0.05 | 0.3703 |
| L HIPP | 0.00 | 0.9674 | 0.09 | 0.2165 | R HIPP | 0.00 | 0.9937 | 0.01 | 0.6859 |
| L DLPFC | 0.00 | 0.9390 | 0.00 | 0.8517 | R DLPFC | 0.00 | 0.9516 | 0.02 | 0.5986 |
| L VTOC | 0.05 | 0.3639 | 0.00 | 0.8709 | R VTOC | 0.02 | 0.5922 | 0.06 | 0.3405 |
| L VWFA | 0.00 | 0.8960 | 0.06 | 0.3168 | R VWFA | 0.02 | 0.5826 | 0.11 | 0.1870 |
| L SMG | 0.00 | 0.8414 | 0.05 | 0.3880 | R SMG | 0.03 | 0.5263 | 0.08 | 0.2477 |
| L AG | 0.00 | 0.9302 | 0.03 | 0.4867 | R AG | 0.01 | 0.7384 | 0.06 | 0.3217 |
| <i>R_{CF}</i> | | | | | | | | | |
| L IPS | 0.08 | 0.2598 | 0.08 | 0.2659 | <i>R IPS</i> | <i>0.55</i> | <i>0.0004</i> | 0.00 | 0.9913 |
| L HIPP | 0.07 | 0.2964 | 0.00 | 0.7900 | R HIPP | 0.37 | 0.0070 | 0.04 | 0.4290 |
| L DLPFC | 0.09 | 0.2247 | 0.01 | 0.6798 | R DLPFC | 0.05 | 0.3659 | 0.00 | 0.9862 |
| L VTOC | 0.09 | 0.2138 | 0.01 | 0.6345 | R VTOC | 0.07 | 0.2917 | 0.00 | 0.9913 |
| L VWFA | 0.05 | 0.3594 | 0.08 | 0.2461 | R VWFA | 0.03 | 0.4802 | 0.07 | 0.2844 |
| L SMG | 0.01 | 0.7741 | 0.01 | 0.7311 | R SMG | 0.02 | 0.6273 | 0.02 | 0.5849 |
| L AG | 0.03 | 0.4983 | 0.00 | 0.9903 | R AG | 0.15 | 0.1152 | 0.07 | 0.2968 |
| <i>R_{GI}</i> | | | | | | | | | |
| L IPS | 0.11 | 0.1863 | 0.00 | 0.8486 | R IPS | 0.03 | 0.5195 | 0.03 | 0.4820 |
| L HIPP | 0.07 | 0.2866 | 0.02 | 0.5509 | R HIPP | 0.01 | 0.7183 | 0.01 | 0.7698 |
| L DLPFC | 0.07 | 0.3042 | 0.00 | 0.9460 | R DLPFC | 0.11 | 0.1752 | 0.03 | 0.4769 |
| L VTOC | 0.26 | 0.0307 | 0.03 | 0.5010 | R VTOC | 0.00 | 0.8141 | 0.10 | 0.2132 |
| L VWFA | 0.04 | 0.4444 | 0.00 | 0.8855 | R VWFA | 0.10 | 0.2008 | 0.01 | 0.7156 |
| L SMG | 0.13 | 0.1396 | 0.01 | 0.7301 | R SMG | 0.03 | 0.4974 | 0.00 | 0.8224 |
| L AG | 0.05 | 0.3563 | 0.07 | 0.2810 | R AG | 0.04 | 0.4414 | 0.00 | 0.8115 |
| <i>R_{SD}</i> | | | | | | | | | |
| L IPS | 0.06 | 0.3369 | 0.01 | 0.6912 | R IPS | 0.15 | 0.1090 | 0.05 | 0.3709 |
| L HIPP | 0.15 | 0.1165 | 0.01 | 0.6868 | R HIPP | 0.08 | 0.2451 | 0.04 | 0.4159 |
| L DLPFC | 0.01 | 0.7443 | 0.00 | 0.9886 | R DLPFC | 0.15 | 0.1105 | 0.13 | 0.1474 |
| L VTOC | 0.00 | 0.8179 | 0.02 | 0.5908 | R VTOC | 0.07 | 0.2919 | 0.00 | 0.9768 |
| L VWFA | 0.11 | 0.1867 | 0.01 | 0.7767 | R VWFA | 0.01 | 0.6585 | 0.01 | 0.7106 |
| L SMG | 0.04 | 0.4560 | 0.05 | 0.3763 | R SMG | 0.01 | 0.7248 | 0.07 | 0.3068 |
| L AG | 0.00 | 0.9240 | 0.06 | 0.3408 | R AG | 0.01 | 0.7139 | 0.01 | 0.7195 |

R_{CT} = change in cortical thickness; *R_{CF}* = change in cortical folding regularity; *R_{GI}* = change in gyrification; *R_{SD}* = change in sulcus depth; L = left hemisphere; R = right hemisphere; IPS = intraparietal sulcus; HIPP = hippocampus; DLPFC = dorso-lateral prefrontal cortex; VTOC = ventral temporal-occipital cortex; VWFA = visual word form area; SGM = supramarginal gyrus; AG = angular gyrus; R² = determinant of covariation.

821